Dipole Dynamics in Liquid Crystalline Epoxies by Broad-Band Dielectric Relaxation Spectroscopy

Jovan Mijovic,* Xiaoya Chen, and Jo-Wing Sy

Department of Chemical Engineering, Chemistry and Materials Science, Polytechnic University, Six Metrotech Center, Brooklyn, New York 11201

Received March 9, 1999; Revised Manuscript Received May 25, 1999

ABSTRACT: Dipole dynamics of a series of thermotropic liquid crystalline (LC) epoxy prepolymers and an LC epoxy/amine network were studied by broad-band dielectric relaxation spectroscopy (DRS) over a wide range of frequency and temperature. Two relaxation processes were observed in the prepolymers below the melting point: the β process, associated with the rotational motions of the LC rigid rods about their molecular axis, and the γ process, whose origin lies primarily in the localized motions of the terminal group. The α process, associated with the segmental motions, emerges as a low-intensity process above the calorimetric glass transition and quickly shifts into the gigahertz frequency range with increasing temperature. The δ process, associated with the end-over-end motions in the mesophase, is largely absent because of a negligible longitudinal dipole moment in these LC epoxy molecules. An in-situ investigation of the formation of an LC epoxy/amine network was conducted by DRS and polarized optical microscopy (POM). The initial stage of cure in the mesophase was characterized by the formation of nematic droplets, which quickly coalesce to form larger structures. An interesting observation was the spontaneous formation and the subsequent change of homeotropic to planar orientation during cure—a trend analogous to that observed by X-ray diffraction. Three relaxations characterize the dynamics of cured networks: the α process due to segmental motions in the cross-linked network, the LC β process also observed in neat prepolymers, and the β_{OH} process, associated with the localized motions of (primarily) hydroxyl groups.

Introduction

There is a considerable current interest in thermotropic liquid crystalline (LC) epoxies, and a number of studies on these materials have been reported in recent years (e.g., refs 1−14), including an excellent review.[15] The introduction of liquid crystallinity adds an important new dimension to the already versatile conventional epoxy networks: the anisotropy of the LC phase leads to an anisotropy of the electrical and optical properties in macroscopically aligned materials that makes them attractive candidates for novel applications in optoelectronic switches, optical filters, displays, sensors, and so on. The majority of the studies thus far have focused on the synthesis of various LC epoxies and their characterization by diverse techniques that include differential scanning calorimetry (DSC), polarized optical microscopy (POM), and X-ray diffraction. Particularly noteworthy contributions to the field were made by Ober and co-workers.[7−9,15] In one of their studies, the cure of an LC epoxy/amine system under applied ac electric field was investigated and the change in the orientation parameter during network formation monitored by the changes in the X-ray diffraction pattern. A change from homeotropic to planar orientation was observed as a result of a shift in the crossover frequency of molecular orientation to lower frequencies in the course of cure. This finding was of great interest to us for both fundamental and applied reasons, the latter having to do with a two-frequency switching ability and an improved switching response in general.[16,17]

However, largely missing from the studies reported hitherto is information about the molecular reorientational dynamics of LC epoxies—an essential element when one considers that the attractiveness of these materials derives largely from the ability of LC molecules to align in response to an applied field. A dielectrically anisotropic phase responds to the applied field to minimize its free energy in the steady field, and if it finds a pathway, a LC material aligns in the field producing a homeotropic or planar sample. The theoretical treatment of dielectric properties of monodomain and polydomain LCs is given in the literature.[18−22] Of the experimental techniques available for the study of reorientational dynamics in molecular liquids, liquid crystals, and polymers, dielectric relaxation spectroscopy (DRS) is rapidly becoming the dominant tool.[23−25] The great potential of DRS derives from an unparalleled frequency range available (12−14 decades) that enables one to probe molecular dynamics of condensed matter in various phases and at different temperature: from amorphous liquids to a liquid crystalline glass; from high temperature, where the dipole relaxation times are of the order of tens of picoseconds, through the vitrification range where the relaxation times in the glass reach tens to hundreds of seconds. There is also a strong practical motivation for the study of dynamics by DRS; consider, for example, that electric field-induced switching of liquid crystal displays is rooted in the anisotropy of the dielectric permittivity—the principal parameter measured by DRS.

In an isotropic amorphous system, with negligible internal field factors, dielectric permittivity is related to the dipole moment correlation function by a Fourier transformation:[26]

$$\frac{\epsilon^*(\omega) - \epsilon_\infty}{\epsilon_0 - \epsilon_\infty} = 1 - i\omega\int_0^\infty [\exp(-i\omega t)]\Phi(t)\,\mathrm{d}t \qquad (1)$$

where ϵ_0 is the limiting low-frequency value of the

* To whom correspondence should be addressed. E-mail jmijovic@poly.edu.

10.1021/ma990354e CCC: $18.00
Published on Web 07/16/1999

dielectric constant, ϵ_∞ is the limiting high-frequency dielectric constant, ω is angular frequency, and $\Phi(t)$ is the relaxation kernel that can be obtained from the dipole correlation function:

$$\Phi(t) = \frac{\sum_i^N \sum_j^N \langle \mu_i(0)\, \mu_j(t) \rangle}{\sum_i^N \sum_j^N \langle \mu_i(0)\, \mu_j(0) \rangle} \tag{2}$$

where $\mu_i(0)$ and $\mu_i(t)$ denote the elementary dipole moment of a molecule i at time $t = 0$ and t, respectively. The correlation function expressed in this form takes into account both equilibrium and dynamic angular correlations between molecules.

Equations 1 and 2 can be generalized further to account for anisotropic LC systems as described in several important contributions by Williams and coworkers.[18−22] For the simple case where the internal field factors are set to unity, two principal complex permittivities $\epsilon_{||}(\omega)$ and $\epsilon_\perp(\omega)$ in an axially symmetric LC phase, which reflects the anisotropy of motions, are written as

$$\frac{\epsilon_\gamma(\omega) - \epsilon_{\infty\gamma}}{\epsilon_{0\gamma} - \epsilon_{\infty\gamma}} = 1 - i\omega F\,[\Phi_{\mu\gamma}(t)] \tag{3}$$

$$[\Phi_{\mu\gamma}(t)] = \frac{\langle \mu_{k\gamma}(0) \cdot \mu_{k\gamma}(t) \rangle}{\langle \mu_{k\mu}{}^2 \rangle} \tag{4}$$

where $\gamma = ||$ or $\perp$. The two permittivities, $\epsilon_{||}(\omega)$ and $\epsilon_\perp(\omega)$, are measured parallel and perpendicular to the principal axis, respectively. For simplicity, only the autocorrelation terms are included in eq 4, although cross-correlation terms can be readily introduced formally for an LC.[22] The form that the correlation function takes in an LC depends on the macroscopic alignment of the sample. Araki et al.[20] have developed a general relationship between the principal complex permittivities and the correlation function for the dipole motion, shown in eqs 5 and 6:

$$\epsilon_{||}(\omega) = \epsilon_{\infty||} + \frac{G}{3kT}[(1 + 2S)\mu_l{}^2\, F_{||}^l(\omega) + (1 - S)\mu_t{}^2\, F_{||}^t(\omega)] \tag{5}$$

$$\epsilon_\perp(\omega) = \epsilon_{\infty\perp} + \frac{G}{3kT}[(1 - S)\mu_l{}^2\, F_\perp^1(\omega) + (1 + S/2)\mu_t{}^2\, F_\perp^t(\omega)] \tag{6}$$

In eqs 5 and 6, μ_l and μ_t are the longitudinal and transverse dipole moments in the mesogens, respectively; G is a term involving the concentration of dipolar mesogenic group; S is the local order parameter, and F is given by the Fourier transform relation:

$$F_j^i(\omega) = 1 - i\omega F\,[F_j^i(t)] \tag{7}$$

Equation 6 reveals that there are four relaxation modes, two involving μ_l and two involving μ_t. Each of the four relaxation modes can be described by a different decay function, F, which in turn is a combination of time correlation functions.[20] The measured permittivity along the direction of the electric field (Z-direction) in an (arbitrarily) macroscopically aligned sample is written as[19]

$$\epsilon_Z(\omega) = \left(\frac{1 + 2S_d}{3}\right)\epsilon_{||}(\omega) + \frac{2}{3}(1 - S_d)\epsilon_\perp(\omega) \tag{8}$$

where S_d is the director order parameter. For a globally unaligned sample, $S_d = 0$, and by making use of eqs 6 and 7, eq 8 is written as

$$\epsilon_Z(\omega) = \epsilon_X(\omega) = \epsilon_Y(\omega)$$

$$= (\epsilon_{\infty||} + 2\epsilon_{\infty\perp})/3 + \frac{G}{9kT}[\mu_l{}^2(1 + 2S)F_{||}^l(\omega) + \mu_t{}^2(1 - S)F_{||}^t(\omega) + 2\mu_l{}^2(1 - S)F_\perp^l(\omega) + 2\mu_t{}^2(1 + S/2)F_\perp^t(\omega)] \tag{9}$$

The results presented in this paper were obtained on the globally disordered samples, and hence eq 9 provides the starting point for our study. Careful inspection of eq 9 reveals that the permittivity, $\epsilon(\omega)$, in globally unaligned sample is a weighted sum of the four relaxation modes (two involve $\mu_{||}$ and two involve $\mu_\perp$). In our samples, however, $\mu_{||}$ is negligibly small due to the symmetry of all the monometic structures (the prepolymers), and hence the relaxation associated with the 00 (the δ process) and the11 modes cannot be observed. Only the 01 and 12 modes will be left to be seen in the dielectric spectra, but these two processes are most likely superposed and should differ from the δ process.

The focus of this study, however, is on a phenomenological description of the reorientational dynamics of LC epoxies. The relaxation kernel, $\phi(t)$, is most often quantified via a stretched exponential function of the Kohlrausch−Williams−Watts[27] (KWW) type:

$$\phi(t) = Ce^{-(t/\tau)^\beta} \tag{10}$$

where C is a constant, τ is the relaxation time, and β is the stretching exponent ranging form 0 to 1. It is sufficient to use only one portion of the real or imaginary permittivity in eq 1, since they are related by the Kramers−Kronig transform, and then by taking the imaginary part of the Fourier transform of eq 2, we obtain

$$\phi(t) = \frac{2}{\pi}\int_0^\infty \frac{\epsilon''(\omega)}{\epsilon_0 - \epsilon_\infty}\frac{\cos(\omega t)}{\omega}\,d\omega \tag{11}$$

However, instead of transforming the frequency domain dielectric data into the time domain using a discrete Fourier transform, where spectral features may be truncated, we transform the relaxation kernel $\phi(t)$ into the frequency domain, using the technique described by Dishon et al.[28] and then fit the experimental data to the transformed kernel with appropriate parameters. Alternatively, ϵ^* may be modeled by a number of empirical functions; a particularly popular and robust form is the Havriliak−Negami [29] (HN) function given as

$$\epsilon^*(\omega) = \epsilon_\infty + \frac{\epsilon_0 - \epsilon_\infty}{[1 + (i\omega\tau_{HN})^a]^b} + i\frac{\sigma}{\omega^n \epsilon_v} \tag{12}$$

where a and b are the dispersion shape parameters, σ is the conductivity, ϵ_v is the vacuum permittivity, and the other parameters are defined in eq 1. Strictly

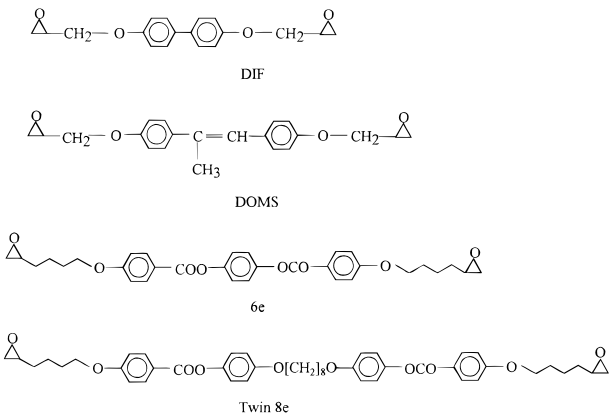

Figure 1. Chemical structure of liquid crystalline (LC) epoxy prepolymers.

speaking, σ is the frequency-independent conductivity only when $n = 1$; for values of n different from unity, the whole second term takes into account conductivity-related processes, such as charge migrations.

In this paper we describe the reorientational dynamics of a series of LC epoxy prepolymers and one LC epoxy/amine formulation during and after cure. The principal objectives of this investigation were (1) to prepare LC epoxies of different liquid crystalline monomeric species (termed here "prepolymers") and elucidate their dynamics in terms of the molecular origin of relaxation processes, the temperature dependence of the most probable relaxation time, and the breadth and shape of the relaxation spectrum and (2) to conduct a preliminary in-situ real time study of cure of LC epoxy networks by DRS.

Experimental Section

Materials. Four thermotropic LC epoxy prepolymers were investigated, and their chemical structures are shown in Figure 1. 4,4′-Diglycidyloxydiphenyl (DIF, EEW = 162 g/mol) was synthesized in our laboratory. A detailed description of the synthesis and characterization of DIF is given elsewhere.[30] The other LC epoxies were synthesized and characterized elsewhere and were supplied to us for this study. 4,4′-Glycidyloxy-α-methylstilbene (DOMS, EEW = 180 g/mol) was obtained from Professor C. Carfagna (University of Naples, Italy). 4-(4-Oxiranylbutoxy)benzoic acid 1,4-phenylene ester (6e, EEW = 278.9 g/mol) and 4-(oxiranylmethoxy)benzoic acid 1,8-octanediylbis(oxy-4,1-phenylene) ester (Twin 8e, EEW = 363.2 g/mol) were supplied by Professor C. K. Ober (Cornell University) and Dr. A. Shiota (Japan Synthetic Rubber Co.). The curing agent, 4,4′-methylenedianiline (MDA), was purchased from Aldrich.

Techniques. Dielectric Relaxation Spectroscopy. A detailed description of our experimental facility for dielectric measurements is given elsewhere,[31,32] and an excellent recap of experimental methodology for dielectric measurements was recently published.[33] However, briefly, we have used a Solartron 1260 FRA with broad-band dielectric converter (Novocontrol GmbH) to cover the frequency range from 1 mHz to 10 MHz, an HP 4284A impedance analyzer to cover the range from 20 Hz to 1 MHz, and an HP 4291A RF impedance analyzer to cover the range from 1 MHz to 1.8 GHz. Supporting evidence was obtained from FTIR, DSC, and POM.

Results and Discussion

In the discussion that follows we concentrate attention on the dielectric response of **6e** (see Figure 1) and then seek to establish the differences and similarities with other LC epoxies in an effort to elucidate the effect of molecular architecture on dynamics. The principal features of the dielectric loss that will be compared are the molecular origin of a relaxation process, relaxation time, shape and breadth of the relaxation spectrum, and dielectric strength. It should be borne in mind that the DRS results described below were obtained in the absence of a directing electric or magnetic field and hence on the samples of spontaneously formed macroscopic alignment.

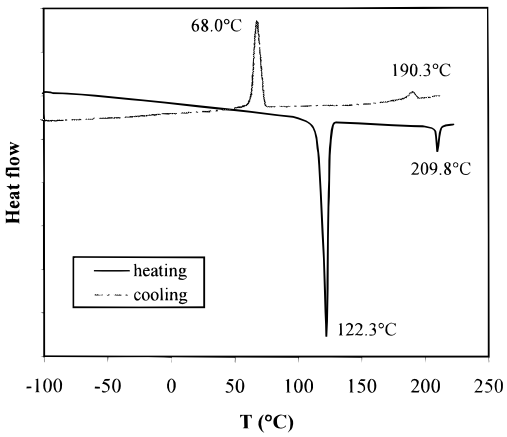

Figure 2. DSC thermogram of **6e**.

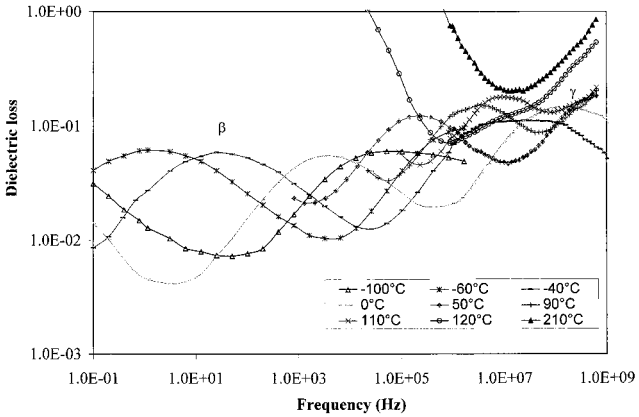

Figure 3. Dielectric loss of **6e** in the frequency domain at selected temperatures during heating.

6e. DSC thermograms of **6e** obtained during heating and cooling are shown in Figure 2. Melting temperature (T_m) and clearing temperature (T_i) are observed in both cases, with each transition appearing at a higher temperature in the heating scan. The appearance of a nematic phase during heating and cooling was confirmed by POM and is described later. DRS results obtained during heating are inspected first. In Figure 3 we show dielectric loss in the frequency domain at a series of selected temperatures. A systematic examination of the data, beginning with low-temperature sweeps, reveals the following. At −100 °C we observe the fast γ process with a peak near 100 kHz (see Figure 3), while only the high-frequency tail of the slower β process is visible at frequencies below 1 Hz. At −60 °C, the γ process moves into the megahertz range, and the β process shifts into our frequency window, with a peak around 1 Hz (see Figure 3). Both γ and β processes are captured in the frequency window of Figure 3 between −40 and 0 °C. With further increase in temperature, however, the γ process moves to frequencies above 1 GHz and out of our range, while the β process also shifts to higher frequency but remains clearly discernible up to approximately 110 °C (Figure 3). A deviation from

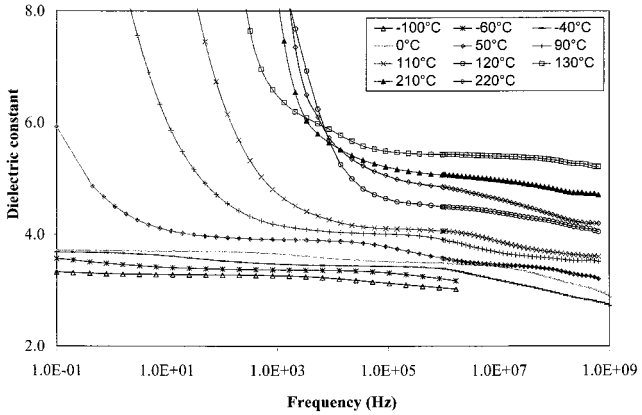

Figure 4. Dielectric constant of **6e** in the frequency domain at selected temperatures during heating.

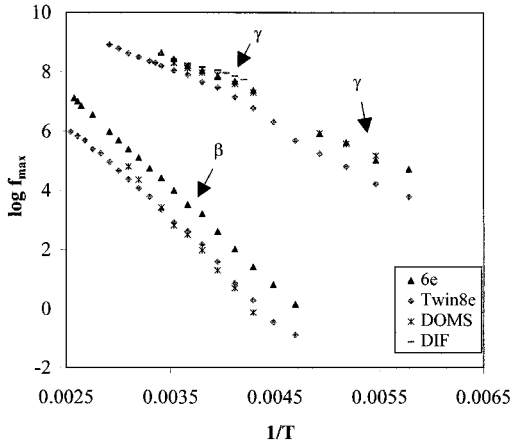

Figure 5. Most probable relaxation time as a function of reciprocal temperature for different prepolymers.

the straight line (conductivity) in the descending portion of the loss curve just before the onset of β relaxation, first seen at 110 °C, is caused by the onset of melting (DSC T_m = 122 °C). Above T_i the conductivity tail bottoms out at about 10 MHz; the α process in the mesophase and in the isotropic liquid ($T > T_i$) is very fast and is located well into the gigahertz range.

An examination of the changes in the dielectric constant is also of interest. The limiting low-frequency value (ϵ_0) increases slowly but gradually during heating from −100 to 110 °C. This is best seen in Figure 4 in the frequency range between approximately 100 kHz and 1 MHz. Melting starts at about 110 °C and is reflected in a significant increase in the dielectric constant (and the conductivity due to migrating charges) between 110 and 130 °C. In the nematic phase, between T_m and T_i, the dielectric constant decreases slightly and then increases abruptly (ca. 10%) in undergoing the nematic-to-isotropic phase transition. In the isotropic state, the dielectric constant decreases with increasing temperature (see e.g. data at 210 and 220 °C in Figure 4).

An examination of the results obtained during cooling yields a similar picture. Following a gradual decrease in temperature from 220 °C (above T_i), we see the first evidence of a relaxation peak below 1 GHz at about 70 °C. On further cooling, γ and β processes enter our frequency window and follow a trend analogous to that observed during heating. The same holds true for the change in the dielectric constant during cooling.

The temperature dependence for τ_{max} ($\tau_{max} = 1/\omega_{max} = {}^1/_2\pi f_{max}$) for β and γ processes during heating and cooling is plotted in Figure 5. Note that Figure 5 is a composite plot for all epoxy prepolymers and, as such, will be invoked repeatedly throughout the text. In **6e**, both processes (β and γ) are characterized by Arrhenius temperature dependence, independent of thermal history (i.e., heating vs cooling). The calculated values are 63 kJ/mol for the β process and 26 kJ/mol for the γ process.

Information on DRS of molecular liquid crystals (MLC) of similar structure is scarce, and the understanding of the various motions involved in the relaxations in LC epoxies was aided by inspecting the reported DRS results for side chain liquid crystalline polymers (SCLCP).[16−26,34−42] It was rationalized that useful information about the molecular origin of a relaxation process in molecular liquid crystals (MLC) can be extracted by comparison with SCLCPs, because the low-temperature dynamics of side chain mesogens are governed by the internal motions that are largely independent of the main chain. Consider, for example, the work of Zentel et al.,[35,36] who studied a series of SCLC acrylates and methacrylates with an ester-linked biphenyl mesogen, i.e., the same unit present in **6e** and **Twin 8e**. They found a β relaxation independent of the type and length of the spacer and assigned this process to the internal motions of the ester moiety in the mesogen. The reported activation energy of approximately 50 kJ/mol was close to the value of 56 kJ/mol calculated by Bormuth et al.[37] for a similar system and the range from 43 to 65 kJ/mol found by Romero Colomer et al.[38] for another series of ester-containing mesogenic units. Previous studies of main chain liquid crystalline polymers (MCLCP) have also confirmed that the local reorientation of −COO− and −C−O−C− dipoles is responsible for β relaxation in these systems.[40] The reported activation energy was between 55 and 59 kJ/mol. The similarity between all those results and our findings suggests that the internal motions of the ester group in the mesogen are at the heart of the β process in **6e** but are not exclusively responsible for it because the contributions from the terminal group on the mesogenic unit and the local mobility of the phenyl group cannot be neglected. Supporting evidence for the effect of the terminal group (e.g., ethoxy vs cyano) was provided by Gedde et al.[41] while the contribution of the local motions by phenyl groups was established by Nikonorova et al.[42] All this suggests that the molecular origin of the β process in **6e** is complex, although it is clear that this relaxation is associated with the rotational motions of the LC rigid rods about their molecular axis and that it involves a multiplicity of dielectrically active motions (mesogen ester, phenyl group, terminal unit). The β process is affected by the glass transition of **6e** (a weak DSC T_g is observed); this is evidenced by a pronounced increase in the intensity of the loss peak above 20 °C (see Figure 3) and a concomitant stepwise increase in the dielectric strength. A further increase in the intensity with increasing temperature is augmented by the overlapping α process, which is similar to the segmental α process in the conventional epoxies and which shifts quickly to higher frequency. The β process is also affected by melting, because the transformation of a three-dimensional crystalline phase into a nematic mesophase is accompanied by a further increase in the mobility of the mesogen about its axis. This is manifested by a shift in the dielectric loss peak into the gigahertz range and a simultaneous increase

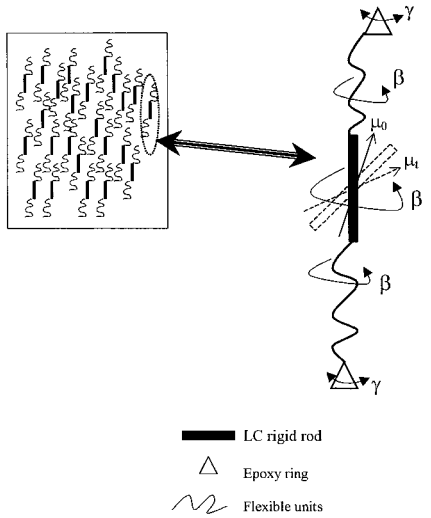

Figure 6. Schematic representation of different molecular motions involved in the dielectric relaxation of LC epoxies. Dash lines represent the rotational motion of LC rigid rod about the molecular long axis.

in the dielectric constant. The γ process has the characteristic features of a fast, localized process; its most probable relaxation time is of the order of 100 ps already at 50 °C (well below the T_m), its intensity increases with increasing temperature, and its activation energy is comparable to that of a local process in non-LC epoxy prepolymers.[43−45] There is little doubt that the origin of γ relaxation in **6e** lies primarily in the localized motions of the terminal group, i.e., the epoxy-capped glycidyl groups. A similar relaxation due to local motions of the terminal substituent was observed in SCLCPs, but only when the terminal group was sufficiently long. For example, the γ process was observed in SCLCPs with butoxy but not cyano or methoxy terminated mesogen.[35,36] The reported activation energy range was 17−24 kJ/mol, in agreement with our value of 26 kJ/mol. Unlike β relaxation, however, the γ process is not uniquely affected by melting because of the localized nature of the motions involved. A schematic presentation of the motions that give rise to γ and β processes in LC epoxy prepolymers is shown in Figure 6.

Both γ and β processes in **6e** are thermodielectrically complex; plots of normalized dielectric loss ($\epsilon''/\epsilon''_{max}$) as a function of normalized frequency (f/f_{max}) did not yield a single master curve. Instead, broader and more asymmetric spectra were observed at higher temperature. The adjustable parameters of the HN equation (eq 5), *a* and *b*, account for the symmetric and asymmetric broadening of the relaxation spectrum, respectively.[46] Excellent HN fits are obtained for the β process, and parameters *a* and *b* are found to vary with temperature; with increasing temperature we observe an increase in *a* (the spectra become narrower) and a decrease in *b* (the spectra become more asymmetric). An examination of the distribution function for the HN equation (the complete expression is given elsewhere[47]) did not provide further insight into the underlying dynamics. The γ process, on the other hand, becomes narrower and more symmetric but cannot be fit very well with a single HN function.

An additional piece of information obtained from DRS is the relaxation strength $\Delta\epsilon = \epsilon_0 - \epsilon_\infty$. The temperature dependence of $\Delta\epsilon$ is often difficult to unambiguously obtain due to a temperature-dependent overlap of two or more relaxation processes. In this case, however, there exists a sufficiently wide range of frequency and temperature where γ and β relaxations can be deconvoluted and their relaxation strengths calculated. The dielectric strength of the γ process (its complexity notwithstanding) was found to increase slightly with increasing temperature—in agreement with the trend observed for localized processes in various amorphous, crystalline, and liquid crystalline materials. The β process, on the other hand, was characterized by a stepwise increase in the dielectric strength around T_g, which is attributed to the added contribution from the α_m process (subscript "m" denotes mesophase) described below.

Dynamics in the LC phase, between T_m and T_i (or T_g and T_i in LCPs), are of interest because the attainment of a reproducible alignment in the mesophase is the key consideration in the application of LC molecules. It is now generally agreed (there is supporting evidence from theory and experiment) that four relaxation modes are possible in unaligned polydomain LC samples and that these modes would give rise to a lower frequency peak due to 00 motion (the δ process) and a broader peak at higher temperature due to a combination of 01, 10, and 11 motions (the α_m process).[48,49] In the absence of a directing electric (or magnetic) field, the measured permittivity corresponds to a weighted sum of the possible relaxation modes possible. The δ process is identified with the 00 rotation of the mesogenic unit relaxing the longitudinal dipole and has been observed, for example, in various cyanobiphenyls.[22] In our LC epoxies, however, the existence of a longitudinal dipole moment is unlikely because of the predominance of the transverse dipole moment in the terminal epoxy groups. In the mesophase, the α_m process observed in our systems has a relaxation time of the order of picoseconds and is located outside the available frequency window. Dynamics in the mesophase are therefore best described by a complex process resulting from the merging of α_m, β, and γ processes. Further information about this complex process was obtained from DRS during cure and is discussed later.

Twin 8e. DSC thermograms of **Twin 8e** also showed two transitions during heating and cooling. Both T_m (149.5 and 108.2 °C during heating and cooling, respectively) and T_i (180.3 and 166.8 °C during heating and cooling, respectively) are lower and the temperature range between them narrower in **Twin 8e** than in **6e**. **Twin 8e** has similar mesogenic structure as **6e** but is a larger molecule (see Figure 1), and it is believed that the eight methylene units between mesogens facilitate the alignment of LC rigid rods. Dielectric loss in the frequency domain with temperature as a parameter, shown in Figure 7, confirms the presence of β and γ processes. The general characteristics of the dielectric response are analogous to those observed in **6e**: the γ process is evident in the temperature range between −100 °C (a broad peak centered at about 10 kHz) and 50 °C. Above that temperature the γ process moves into the gigahertz range. The slower β process is first seen at −50 °C, with a peak just below 1 Hz. One major difference between **6e** and **Twin 8e** is the observed difference in the intensities of β and γ processes, which is more pronounced in **Twin 8e**, as evidenced by contrasting Figures 3 and 7. An increase in the difference in the intensities of γ and β processes in **Twin 8e** relative to **6e** derives from (1) a decrease in the intensity

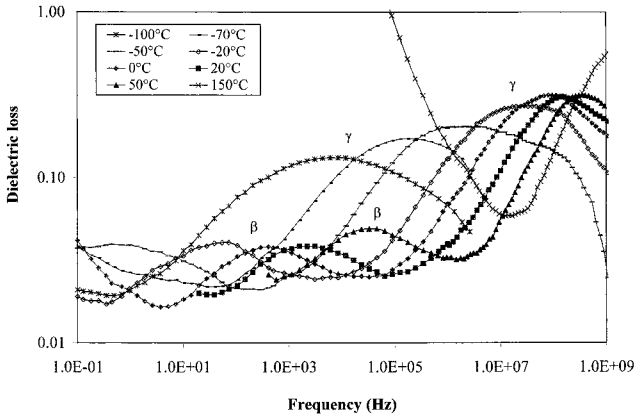

Figure 7. Dielectric loss of **Twin 8e** in the frequency domain at selected temperatures during heating.

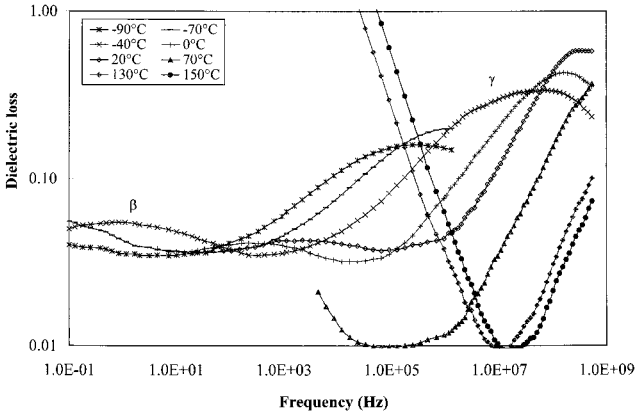

Figure 8. Dielectric loss of **DOMS** in the frequency domain at selected temperatures during heating.

of the β process due to a decrease in concentration of ester groups per unit volume and (2) an increase in the intensity of the γ process in **Twin 8e** for the reasons described below. An examination of the results obtained during cooling yields a similar picture.

Although the molecular origins of γ and β processes (i.e., localized motions and motions of rigid rods, respectively) in **Twin 8e** and **6e** are fundamentally similar, the dielectric response of these two LC epoxies is not identical because of the difference in the molecular architecture. The temperature dependence for τ_{max} for β and γ processes during heating and cooling is shown in Figure 5. The β process is characterized by Arrhenius temperature dependence, independent of thermal history. The calculated value of 63 kJ/mol is identical to that found in **6e**. The slightly lower intensity is due to the lower concentration of mesogen esters per unit volume. The γ process in **Twin 8e** is much more pronounced, and it appears to be characterized by two distinct slopes in the relaxation map, with activation energies of 36 and 18 kJ/mol for the low- and high-temperature range, respectively. Useful information about the origin of the motions involved is again deduced by invoking analogy with SCLCPs, where, in several instances, two γ relaxations were observed below the glass transition. These two processes, termed γ_1 and γ_2 on the order of increasing frequency, were reported to have an activation energy between 34 and 40 and 17−24 kJ/mol, respectively. The γ_1 process in **Twin 8e** is associated with the $-O-(CH_2)_8-O-$ unit. In support of this assignment we cite the report of local motions in polyethers $[-(CH_2)_i-O-, i > 4)]$, with an activation energy of 40 kJ/mol,[50] and in a SCLCP with a long spacer $[-(CH_2)_{11}-]$, with an activation energy of 34 kJ/mol.[40] The γ_2 process in **Twin 8e** is caused by the localized motions of the terminal group. The limiting low-frequency value of the dielectric constant (ϵ_0) increases slowly but gradually with increasing temperature between −100 °C and T_m, independent of thermal history. This is best seen in the frequency domain in the range between 100 kHz and 1 MHz but could be also observed in a temperature scan at a constant frequency. Melting is accompanied by a significant increase in the dielectric constant. Above T_i, however, the dielectric constant decreases with a further increase in temperature.

The γ and β processes in **Twin 8e** are also thermodielectrically complex. The plots of normalized dielectric loss ($\epsilon''/\epsilon''_{max}$) for the γ process as a function of normalized frequency (f/f_{max}) do not fall on a single master curve; broader and more asymmetric spectra are obtained at lower temperature.

DOMS. The general features of **DOMS** obtained from DSC and DRS are similar to those of **6e** and **Twin 8e**. DSC thermograms of **DOMS** also showed two transitions during heating and cooling: T_m (82 and 64.5 °C during heating and cooling, respectively) and T_i (131 and 105.3 °C during heating and cooling, respectively). **DOMS** is reportedly a monotropic nematogen; a POM study revealed a nematic phase with a transition enthalpy of 3.3 J/g measured by DSC. Dielectric loss in the frequency domain during heating with temperature as a parameter is shown in Figure 8. It is interesting to point out that the difference in the intensities of γ and β processes in **DOMS** is quite similar to that of **Twin 8e**.

The temperature dependence for τ_{max} for β and γ processes during heating and cooling is shown in Figure 5. The β process is characterized by Arrhenius temperature dependence, independent of thermal history. The calculated value of 73 kJ/mol is higher than in **6e** and **Twin 8e**, probably because the rotation of the mesogen around its molecular long axis is more difficult in **DOMS** and hence requires higher activation energy. The intensity of β relaxation is lower than in **6e** or **Twin 8e** because of the low polarity (a weak dipole moment is contributed by the asymmetric double bond) in the mesogen unit, which leaves the ether oxygen and terminal groups as principal sources of dipolar contribution to the β process. The γ process in **DOMS** has the same molecular origin as in **6e** and **Twin 8e**, i.e., the localized motions of epoxy-capped glycidyl groups. The variation in the dielectric constant with temperature parallels the trend observed in **Twin 8e**.

It is useful to compare the dielectric strength for γ and β processes as a function of temperature in **6e**, **Twin 8e**, and **DOMS**. The highest intensity γ process is observed in **DOMS**, and that is attributed to the highest concentration of terminal epoxy groups per unit volume. The γ process is more intense in **Twin 8e** than **6e** because of the contribution from the $-O-(CH_2)_8-O-$ unit. The β process is of similar intensity in all samples and varies little with temperature, except for a stepwise increase following the glass transition.

DIF. The dielectric response of **DIF** was somewhat different from the other LC epoxy prepolymers. T_m and T_i, observed in a DSC thermogram during cooling, were quite close to one another: T_m = 134 °C; T_i = 146 °C. Only T_m = 151 °C was observed during heating. Dielectric loss in the frequency domain with tempera-

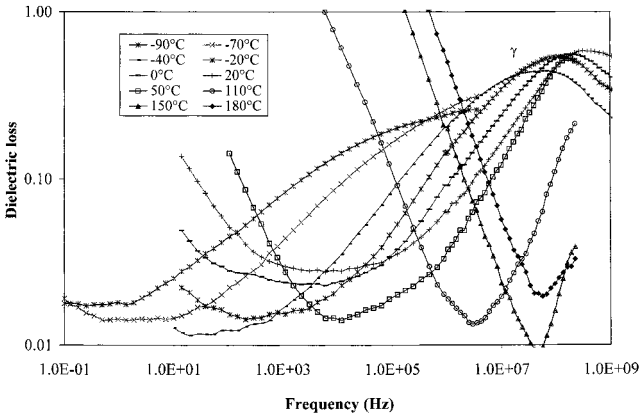

Figure 9. Dielectric loss of **DIF** in the frequency domain at selected temperatures during heating.

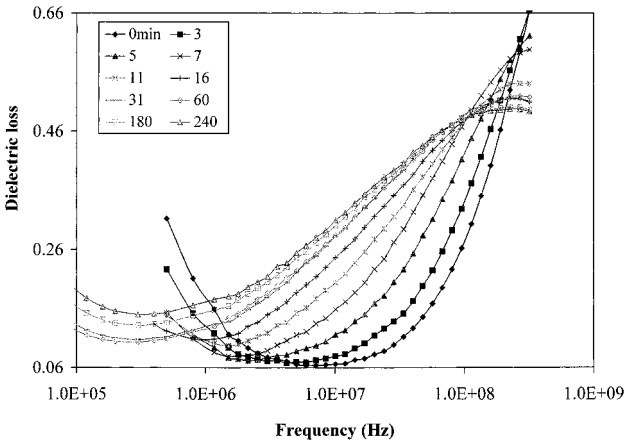

Figure 10. Dielectric loss in the frequency domain for **6e/MDA** formulation during cure at 140 °C.

ture as a parameter, shown in Figure 9, suggests the presence of only one relaxation process. We term it γ, because of the similarity to that process in other LC epoxies, and examine its evolution beginning with low-temperature sweeps. At −100 °C we observe a very broad relaxation peak that spans the entire frequency window of Figure 9. With increasing temperature this peak shifts to higher frequency, increases in intensity, and becomes narrower. Above approximately 50 °C, the peak maximum moves out of the frequency window of Figure 9 and into the gigahertz range. A careful examination of Figure 9 reveals the presence of a plateau in the loss (see e.g. data at 0 and 20 °C) at the low-frequency end of the γ process, suggesting a possible presence of a slower process. Unfortunately, the conductivity due to migrating charges is quite high in this sample, and that precludes further identification (or physically meaningful deconvolution) of such a process. Similar results were obtained during cooling. The temperature dependence for τ_{max} for the γ process during heating and cooling is Arrhenius-like and independent of thermal history. The calculated activation energy of 18 kJ/mol is similar to those found in other LC epoxy prepolymers. We have also observed a systematic increase in the dielectric constant with increasing temperature during heating and cooling.

DRS during Network Formation. Our next goal was to build on our recent work on conventional epoxy/amine networks[51] and conduct a preliminary DRS investigation of the effect of cure on the dynamics of an LC epoxy/amine formulation. It was anticipated that such information would usher the way for the subsequent development of a methodology to correlate chemical kinetics and molecular dynamics in LC networks. The system under investigation was composed of the stoichiometric amounts of **6e** and **MDA**, and the cure was studied under isothermal conditions at 140 °C. The selected formulation and the curing conditions were identical to those used by Ober and Shiota,[8] who monitored the change in the orientation parameter during cure by X-ray diffraction. It was believed that DRS would yield valuable complementary information.

In Figure 10 we show dielectric loss in the frequency domain with cure time as a parameter. It is immediately clear from this figure that all relaxation processes in the initial mixture (0% conversion) at 140 °C are located well into the gigahertz range, and it was not until about 30 min of cure that a broader and less intense loss peak moved into our frequency window. Subsequent cure had little effect on this relaxation, and the completion of chemical reactions after approximately 30 min at 140 °C was confirmed by DSC and FTIR. An important consideration is the molecular origin of this relaxation. Individually, at 140 °C neat **6e** is in the mesophase, where α_m, β, and γ relaxations are active, while **MDA** has its own α process. If and how these molecular motions are affected by mixing at 140 °C is not clear because they overlap, and their locations remain well above 1 GHz. This was unfortunate considering that our initial strategy for quantitative analysis of cure by DRS called for the use of the frequency of the maximum loss, f_{max}, and the corresponding time, t_{max}, as operational parameters that would relate chemical kinetics to molecular dynamics. The inability to monitor the entire loss spectrum from the onset of cure rendered this approach arbitrary (curve fitting after approximately 15 min of cure is possible but physically unsound). An alternative route consists of tracking the changes in the limiting low-frequency dielectric constant (ϵ_0'), obtained by the extrapolation of the value immediately preceding the onset of relaxation. This extrapolated value of ϵ_0' at any time during cure is a function of degree of cure but not frequency. By assuming that the limiting high-frequency dielectric constant (ϵ_∞') does not vary with cure and by subtracting it from ϵ_0', one can calculate the dielectric strength at any given time during cure. The dielectric strength, on the other hand, is related to the effective dipole moment, which, in turn, is a function of the concentration of dielectrically active groups. By monitoring the disappearance of such (reactive) groups during cure (i.e., the change in concentration by FTIR), it becomes possible to relate the change in ϵ_0' (and/or dielectric strength) to the change in the effective dipole moment and hence to quantify the progress of cure. An additional consideration in LC molecules is the effect of orientation (e.g., transition from homeotropic to planar) and that must be accounted for in the analysis. Although we made no attempts at such analysis, we did perform a simultaneous investigation of cure by polarized optical microscopy (POM), and that proved most revealing. The sequence of micrographs shown in Figure 11A−F describes a remarkable change in texture during cure at 140 °C. The initial texture (Figure 11A) is that of nematic droplets, which are known to characterize the nematic phase of MLCs and LCPs.[52] The early stages of cure are accompanied by the coalescence of some droplets and the formation of larger structures (Figure 11B). After approximately 2−3 min we observe the Schlieren and homeotropic textures; the latter are

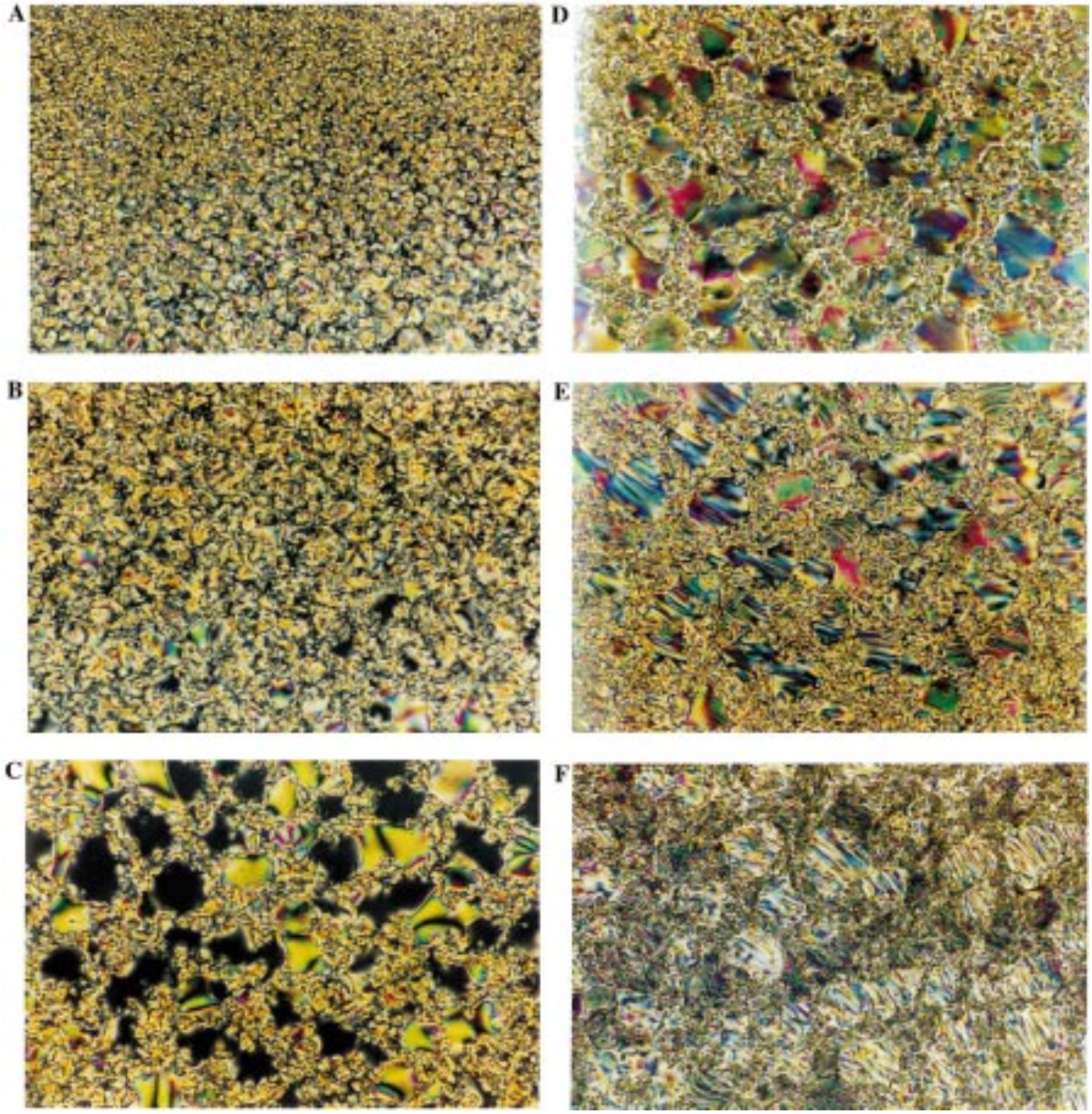

Figure 11. Polarized optical micrographs of **6e/MDA** formulation during cure at 140 °C: (A) $t = 0$ min, (B) $t = 1$ min, (C) $t = 3$ min, (D) $t = 18$ min, and (E) $t = 180$ min; (F) $t = 180$ min, $T = 25$ °C. Scale: 1 cm = 66 μm.

a result of spontaneous orientation in the mesophase and appear as dark areas (Figure 11C) because the director is parallel to the light beam.[52−54] After approximately 12 min these dark areas become gradually lighter before attaining a brightly colored appearance (Figure 11D). One significant finding is that the observed variation in texture, as the black areas turn brightly colored, parallels the change from homeotropic to planar orientation in this system (under the same cure conditions) observed by X-ray diffraction.[8] No further change in texture was observed beyond 18 min of cure at 140 °C (Figure 11E). An essentially identical texture was observed in the glassy nematic (DSC T_g = 71 °C) upon cooling from 140 C to 20 °C (Figure 11F).

DRS of Cured Network. Further information about the dynamics of a cured network was obtained from the frequency sweeps at selected isothermal steps during gradual cooling from 140 to −100 °C. Figure 12 shows dielectric loss in the frequency domain for fully cured (at 140 °C) **6e/MDA** at selected temperatures. Consider as the starting point the relaxation process in a cured network, centered around 100 MHz at 140 °C. At that temperature, the relaxation peak encompasses three

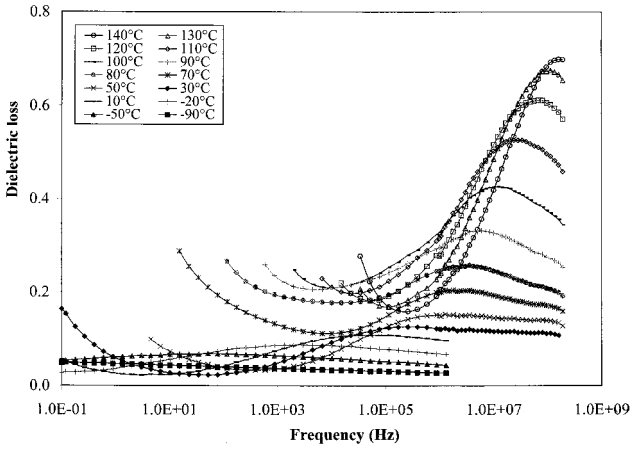

Figure 12. Dielectric loss in the frequency domain for **6e/MDA** at selected temperatures following the cure at 140 °C.

overlapping processes. These are, on the order of increasing frequency, (1) the α process, due to segmental motions in the cross-linked LC network (also present in conventional epoxy networks); (2) the LC β process, due to the motions associated with the mesogen and described in detail earlier in the text; and (3) the β_{OH} process, associated with the localized motions due to (primarily) hydroxyl groups (also present in conventional epoxy networks). The likelihood of end-over-end motions that give rise to the δ process is negligible in neat **6e** and nil in the cured (cross-linked) network. The fast γ process is not present in the cured network because the epoxy groups are consumed during cure. With decreasing temperature we observe an increase in the most probable relaxation time for this complex process ($\alpha\beta\beta_{OH}$) and an increase in the breadth of the relaxation peak. A dramatic decrease in the loss peak height with temperature reflects a general decrease in the extent of dipolar motions, in orientational space, with decreasing temperature. Simultaneously, a pronounced drop in the dielectric strength was noted around the network T_g, detected by DSC at 71 °C. Unfortunately, the α process cannot be deconvoluted meaningfully—its intensity is low, and it shifts quickly to lower frequency with decreasing temperature. Since the α process is associated with the network T_g (71 °C), its relaxation time should be of the order of seconds to hundreds of seconds (i.e., below 1 Hz), but at those frequencies high conductivity dominates the dielectric response. The $\beta-\beta_{OH}$ splitting is first seen at about 110 °C, and it becomes more pronounced with decreasing temperature. The activation energy for β relaxation below T_g (where deconvolution is physically sound) is 66 kJ/mol, practically identical to the value found in neat **6e**.

Summary and Conclusions

Dielectric relaxation spectroscopy (DRS) of a series of thermotropic liquid crystalline (LC) epoxy prepolymers has provided important information about the molecular dynamics of these molecules. Two relaxation processes, β (lower frequency) and γ, are active below the melting point. The molecular origin of the β process is complex, although it is clear that this relaxation is associated with the rotational motions of the LC rigid rods about their molecular axis and that it involves a multiplicity of dielectrically active motions (mesogen ester, phenyl group, terminal unit). The origin of γ relaxation lies primarily in the localized motions of the terminal group, i.e., the epoxy-capped glycidyl groups, with an added contribution form the polyether units that are present in one prepolymer. The dynamics in the mesophase are dominated by a segmental α type process, which encompasses various motions predominately associated with the transverse component of the molecular dipole moment. The absence of the longitudinal dipole moment in these LC epoxy prepolymers is the reason for the absence of the δ process associated with the end-over-end motions. The α process is very fast, and its most probable relaxation time above the melting point is of the order of picoseconds.

The evolution of network formation during the isothermal cure of an LC epoxy/amine formulation was tracked by DRS and optical microscopy. The initial texture is that of nematic droplets, which are known to characterize the nematic phase of MLCs and LCPs. The early stages of cure are accompanied by the coalescence of some droplets and the formation of larger structures. After approximately 2−3 min we observe the Schlieren and homeotropic textures, the latter resulting from spontaneous orientation in the mesophase. After approximately 12 min the dark areas that correspond to the homeotropic texture become gradually lighter before attaining a brightly colored appearance. A significant finding is that the observed variation in texture, as the black areas turn brightly colored, is in complete agreement with the conclusions of Shiota and Ober,[8] who recorded the change from homeotropic to planar orientation in this system (under the same cure conditions) by X-ray diffraction. No further change in texture was observed beyond 18 min of cure at 140 °C, and an essentially identical texture was observed in the glassy nematic network.

Acknowledgment. This material is based on work supported by the National Science Foundation under Grants DMR-9710480 and INT-9724714. We are grateful to Mino Carfagna and A. Shiota for supplying the samples and to Chris Ober for helpful discussions.

References and Notes

(1) Barclay, G. G.; Ober, C. K.; Papathomas, K. I.; Wang, D. W. *J. Polym. Sci., Part A: Polym. Chem.* **1992**, *30*, 1831.
(2) Su, W.-F. A. *J. Polym. Sci., Part A: Polym. Chem.* **1993**, *31*, 3251.
(3) Carfagna, C.; Amendola, E.; Giamberini, M.; Filippov, A. G.; Bauer, R. S. *Liq. Cryst.* **1993**, *13* (4), 571.
(4) Amendola, E.; Carfagna, C.; Giamberini, M.; Pisaniello, G. *Macromol. Chem. Phys.* **1995**, *196*, 1577.
(5) Heberer, D.; Keller, A.; Percec, V. *J. Polym. Sci., Part B: Polym. Phys.* **1995**, *33*, 1877.
(6) Mormann, W.; Brocher, M. *Macromol. Chem. Phys.* **1996**, *197*, 1841.
(7) Shiota, A.; Ober, C. K. *Polymer* **1997**, *38* (23), 5857.
(8) Shiota, A.; Ober, C. K. *Macromolecules* **1997**, *30*, 4278.
(9) Shiota, A.; Ober, C. K. *J. Polym. Sci., Part B: Polym. Phys.* **1998**, *36*, 31.
(10) Ortiz, C.; Kim, R.; Rodighiero, E.; Ober, C. K.; Kramer, E. J. *Macromolecules* **1998**, *31*, 4074.
(11) Liu, J.; Wang, C.; Campbell, G. A.; Earls, J. D.; Priester, R. D. *J. Polym. Sci., Part A: Polym. Chem.* **1997**, *35*, 1105.
(12) Lin, Q.; Yee, A. F.; Sue, H.-J.; Earls, J. D.; Hefner, R. E. *J. Polym. Sci., Part B: Polym. Phys.* **1997**, *35*, 2363.
(13) Sue, H.-J.; Earls, J. D.; Hefner, R. E.; Villarreal, M. I.; Garcia-Meitin, E. I.; Yang, P. C.; Cheatham, C. M.; Plummer, C. J. G. *Polymer* **1998**, *39* (20), 4707.
(14) Benicewicz, B. C.; Smith, M. E.; Earls, J. D.; Priester, R. D.; Setz, S. M.; Duran, R. S.; Douglas, E. P. *Macromolecules* **1998**, *31*, 4730.
(15) Shiota, A.; Ober, C. K. *Prog. Polym. Sci.* **1997**, *22*, 975.
(16) Araki, K.; Attard, G. S. *Liq. Cryst.* **1986**, *1*, 301.
(17) Nazemi, A.; Kellar, E. J. C.; Williams, G.; Karasz, F. E.; Hill, J. S.; Lacey, D.; Gray, G. W. *Liq. Cryst.* **1991**, *9*, 307.
(18) Attard, G. S.; Araki, K.; Willams, G. *J. Mol. Electron.* **1987**, *3*, 1.
(19) Attard, G.; Araki, K.; Williams, G. *Br. Polym. J.* **1987**, *19*, 119.
(20) Araki, K.; Attard, G. S.; Kozak, A.; Williams, G.; Gray, G. W.; Lacey, D.; Nestor, G. *J. Chem. Soc., Faraday Trans. 2* **1988**, *84*, 1067.
(21) Kozak, A.; Moscicki, J. K.; Williams, G. *Mol. Cryst. Liq. Cryst.* **1991**, *201*, 1.
(22) Williams, G. In *The Molecular Dynamics of Liquid Crystals*; Luckhurst, G., Veracini, C., Eds.; Kluwer Academic: Dordrecht, 1994; p 431.
(23) Williams, G. In *Keynote Lectures in Selected Topics of Polymer Science*; Riande, E., Ed.; CSIC: Madrid, 1997; Chapter 1, p 1.
(24) Williams, G. In *Dielectric Spectroscopy of Polymeric Materials: Fundamentals and Application*; Runt, J. P., Fitzgerald, J. J., Eds.; American Chemical Society: Washington, DC, 1997; Chapter 1, p 3.
(25) Simon, G. P. In *Dielectric Spectroscopy of Polymeric Materials: Fundamentals and Application*; Runt, J. P., Fitzgerald,

J. J., Eds.; American Chemical Society: Washington, DC, 1997; Chapter 15, p 329.
(26) Williams, G. In *Comprehensive Polymer Science*; Allen, G., Bevington, J. C., Eds.; Pergamon Press: London, 1988; Vol. 2, Chapter 18, pp 601−632.
(27) Williams, G.; Watts, D. C. *Trans. Faraday Soc.* **1970**, *66*, 80.
(28) Dishon, M.; Weiss, G. H.; Bendler, J. T. *J. Res. Nat. Bur. Stand.* **1985**, *90*, 27.
(29) Havrilliak, S.; Negami, S. *J. Polym. Sci., Part C* **1966**, *14*, 99.
(30) Chen, X. Relaxation Phenomena in Liquid Crystalline Epoxies by Dielectric Relaxation Spectroscopy. M.S. Thesis, Polytechnic University, New York, 1998.
(31) Fitz, B.; Andjelic, S.; Mijovic, J. *Macromolecules* **1997**, *30*, 5227.
(32) Fitz, B.; Mijovic, J. Segmental Dynamics in Poly(methylphenylsiloxane) Networks by Dielectric Relaxation Spectroscopy. *Macromolecules*, in press.
(33) Kremer, F. In *Dielectric Spectroscopy of Polymeric Materials: Fundamentals and Application*; Runt, J. P., Fitzgerald, J. J., Eds.; American Chemical Society: Washington, DC, 1997; Chapter 15, p 423.
(34) Kresse, H.; Kostromin, S.; Shibaev, V. P. *Makromol. Chem. Rapid Commun.* **1982**, *3*, 509.
(35) Zentel, R.; Strobl, G.; Ringsdorf, H. In *Recent Advances in Liquid Crystalline Polymers*; Chapoy, L. L., Ed.; Elsevier: London, 1985; Chapter 17.
(36) Zentel, R.; Strobl, G.; Ringsdorf, H. *Macromolecules* **1985**, *18*, 960.
(37) Bormuth, F. J.; Biradar, A. M.; Quotschalla, U.; Haase, W. *Liq. Cryst.* **1989**, *5*, 1549.
(38) Romero Colomer, F.; Meseguer Duenas, J. M.; Gomez Ribelles, J. L.; Barrales-Rienda, J. M.; Bautista de Ojeda, J. M. *Macromolecules* **1993**, *26*, 155.
(39) Attard, G. S.; Williams, G.; Gray, G. W.; Lacey, D.; Gemmel, P. A. *Polymer* **1996**, *27*, 185.
(40) Blundell, D. J.; Buckingham, K. A. *Polymer* **1985**, *26*, 1623.
(41) Gedde, U. W.; Liu, F.; Hult, A.; Sahlen, F.; Boyd, R. H. *Polymer* **1994**, *35*, 2056.
(42) Nikonorova, N. A.; Borisova, T. I.; Burshtein, L. L.; Freidzon, Ya. S.; Shibaev, V. P. *Polym. Sci. USSR* **1990**, *32*, 82.
(43) Fitz, B.; Andjelic, S.; Mijovic, J. *Macromolecules* **1997**, *30*, 5239.
(44) Corezzi, S.; Capaccioli, S.; Gallone, G.; Livi, A.; Rolla, P. A. *J. Phys.: Condens. Matter* **1997**, *9*, 6199.
(45) Pochan, J. M.; Gruber, R. J.; Pochan, D. F. *J. Polym. Sci. Polym. Phys. Ed.* **1981**, *19*, 143.
(46) It is readily seen that the Havriliak−Negami equation is a generalization of the Cole−Cole equation, to which it reduces for $b = 1$, and a generalization of the Cole−Davidson equation, to which it reduces for $a = 1$.
(47) Bottcher, C. J. F.; Bordewijk, P. *Theory of Electric Polarization, II. Dielectrics in Time-Dependent Fields*, 2nd ed.; Elsevier: Amsterdam, 1978.
(48) Attard, G. S. *Mol. Phys.* **1986**, *58*, 1087.
(49) Moscicki, J. K. In *Liquid Crystal Polymers: From Structures to Applications*; Collyer, A. A., Ed.; Elsevier Appl. Sci.: London, 1992; Chapter 4, p 143.
(50) McCrum, N. G.; Read, B. E.; Williams, G. *Anelastic and Dielectric Effects in Polymeric Solids*; Wiley: New York, 1967.
(51) Andjelic, S.; Mijovic, J. *Macromolecules* **1998**, *31*, 8463.
(52) Noel, C.; Friedrich, C.; Leonard, V.; Le Barny, P.; Ravaux, G.; Dubois, J. C. *Makromol. Chem. Macromol. Symp.* **1989**, *24*, 283.
(53) Noel, C. In *Liquid Crystal Polymers: From Structures to Applications*; Collyer, A. A., Ed.; Elsevier Appl. Sci.: London, 1992.
(54) Noel, C. In *Side Chain Liquid Crystal Polymers*; McArdle, C. B., Ed.; Blackie and Son Ltd.: Glasgow, 1989; Chapter 6, p 159.

MA990354E